N O T I C E

THIS DOCUMENT HAS BEEN REPRODUCED FROM MICROFICHE. ALTHOUGH IT IS RECOGNIZED THAT CERTAIN PORTIONS ARE ILLEGIBLE, IT IS BEING RELEASED IN THE INTEREST OF MAKING AVAILABLE AS MUCH INFORMATION AS POSSIBLE

NASA
Technical Memorandum 82622

AVRADCOM
Technical Report 81-C-13

Surface Geometry of Circular Cut Spiral Bevel Gears

R. L. Huston
University of Cincinnati
Cincinnati, Ohio

and

John J. Coy
Propulsion Laboratory
AVRADCOM Research and Technology Laboratories
Lewis Research Center
Cleveland, Ohio

Prepared for the
Design Engineering Technical Conference
sponsored by the American Society of Mechanical Engineers
Hartford, Connecticut, September 20-23, 1981

NASA

SURFACE GEOMETRY OF CIRCULAR CUT SPIRAL BEVEL GEARS

R. L. Huston*
University of Cincinnati
Department of Mechanical Engineering
Cincinnati, Ohio 45221

and

J. J. Coy*
Propulsion Laboratory
AVRADCOM Research and Technology Laboratories
NASA Lewis Research Center
Cleveland, Ohio 44135

E-873

ABSTRACT

An analysis of the surface geometry of spiral bevel gears formed by a circular cutter is presented. The emphasis is upon determining the tooth surface principal radii of curvature of crown (flat) gears. Specific results are presented for involute, straight, and hyperbolic cutter profiles. It is shown that the geometry of circular cut spiral bevel gears is somewhat simpler than a theoretical logarithmic spiral bevel gear.

INTRODUCTION

In a recent paper [1]** the fundamental geometrical characteristics of theoretical spiral bevel gear tooth surfaces were studied and discussed with particular emphasis given to the determination of the principal radii of curvature. Such an analysis provides a point of departure for the study of contact stresses, lubrication, wear, fatigue life, and gearing kinematics. However, the theoretical gears studied in [1] have a tooth centerline in the shape of a logarithmic spiral, and are, therefore, diffucult to manufacture. (A logarithmic spiral has the property that all radial lines intersect the curve at a constant angle. This leads to a uniformly shaped profile of the gear tooth in the tangential planes of the gear, thus providing

---

*Member ASME.

**Numbers in brackets refer to references at the end of the paper.

for uniform meshing kinematics.) To overcome the fabrication difficulties, gear manufacturers have approximated the logarithmic spiral with a circle, leading to the widely used "circular-cut" spiral bevel gears. Indeed, probably more than 90 percent of the spiral bevel gears in use today are manufactured with a circular cutter. Moreover, Buckingham [2] has observed that, within reasonable limits, a logarithmic spiral and a nearly concentric circle differ by less than $\pm 6^\circ$ in the inclination of their tangent lines - although with some applications this difference may be very significant. Therefore, the objective of this paper is to present an analysis of the geometrical characteristics of these circular cut gears. As in [1] the emphasis is the determination of the surface principal radii of curvature. To keep the analysis as simple and as fundamental as possible, the discussion is restricted to crown gears (i.e., flat gears) which form the so-called "crown rack" of spiral bevel gears. Procedures for manufacturing such gears are found in Refs. [3-7].

NOMENCLATURE

$\underset{\sim}{e}_i (i = 1,2)$	surface base vectors
g	determinant of g_{ij}
$g_{ij} (i,j = 1,2)$	metric tensor coefficients
$\underset{\sim}{h}_i (i = 1,2)$	fundamental vector defined by Eq. (5)
$h_{ij} (i,j = 1,2)$	second fundamental tensor defined by Eq. (6)
$\underset{\sim}{n}$	unit vector normal to surface
$\underset{\sim}{n}_c$	see Fig. 3
$\underset{\sim}{n}_r$	radial unit vector (Fig. 3)
$\underset{\sim}{n}_t$	see Fig. 3
$\underset{\sim}{n}_x, \underset{\sim}{n}_y, \underset{\sim}{n}_z$	unit vectors parallel to XYZ
r	radius of surface of revolution, radial distance

u_1, u_2	surface defining parameters
x, y, z	coordinates of P relative to X,Y,Z
$\hat{x}, \hat{y}, \hat{z}$	coordinates relative to X,Y,Z
C	curve defining surface of revolution; cutter center (see Fig. 5)
H,V	coordinates of Q (see Fig. 7)
J	mean curvature
K	Gaussiasn curvature
N	normal line to surface of resolution
O	origin of XYZ axis system (see also Fig. 3)
O_c	center of involute generating circle
P	typical point on surface
$\underset{\sim}{P}$	position vector to a typical point on surface
P_m	midpoint of crown gear tooth
Q	see Fig. 3
R	radial line (see Fig. 2)
R_c	distance CP_m (see Fig. 7), cutter radius (see Fig. 6)
R_1, R_2	principal radii of curvature
S	general surface
T	tangent line to C, tangent point
X,Y,Z	mutually perpendicular coordinate-axis sytem
$\hat{X}, \hat{Y}, \hat{Z}$	mutually perpendicular coordinate-axis system (see Fig. 7)
θ	angle between R and X-axis, pressure angle (see Figs. 6 and 7)
ϕ	angle between N and Z-axis
ψ	inclination angle of T (see Fig. 1), spiral angle (see Fig. 7)

PRELIMINARY CONSIDERATIONS

Differential Geometry Formulae

Since the principal radii of curavature of a gear tooth surface at a point are among the major factors affecting the lubrication, surface fatigue, contact stress, wear, and life of the gear, it is helpful to summarize the basic formulae from elementary differential geometry which may be used to determine these radii of curvature.

Suppose a surface S is defined by a pair of parameters u_1 and u_2 through the vector parametric equation $\underset{\sim}{P} = \underset{\sim}{P}(u_1,u_2)$ where $\underset{\sim}{P}$ is the position vector of a typical point P on S. Then base vectors $\underset{\sim}{e}_i (i = 1,2)$ tangent to S at P are given by

$$\underset{\sim}{e}_i = \partial \underset{\sim}{P}/\partial u_i \qquad i = 1,2 \tag{1}$$

A surface metric tensor $g_{ij}(i,j = 1,2)$ may then be defined as

$$g_{ij} = \underset{\sim}{e}_i \cdot \underset{\sim}{e}_j \tag{2}$$

Let g be the determinant of g_{ij}. Then it is easily shown that

$$\sqrt{g} = \left| \underset{\sim}{e}_1 \times \underset{\sim}{e}_2 \right| \tag{3}$$

Hence, a unit vector $\underset{\sim}{n}$ normal to S is then

$$\underset{\sim}{n} = \underset{\sim}{e}_1 \times \underset{\sim}{e}_2/\sqrt{g} \tag{4}$$

Let the fundamental vector $\underset{\sim}{h}_i (i = 1,2)$ be defined as

$$h_i = \partial \underset{\sim}{n}/\partial u_i \tag{5}$$

Then, the second fundamental tensor $h_{ij}(i,j = 1,2)$ is defined as

$$h_{ij} = -\underset{\sim}{h}_i \cdot \underset{\sim}{e}_j \tag{6}$$

Letting h be the determinant of h_{ij}, the Gaussian curvature K is defined as

$$K = h/g \tag{7}$$

A positive Gaussian curvature indicates that all points in the surface in the neighborhood of P lie on the same side of a plane tangent to the surface. Let $k_{ij}(i,j = 1,2)$ be defined as

$$k_{ij} = g^{-1}_{i\ell} h_{\ell j} \tag{8}$$

where g^{-1}_{ij} is the inverse of g_{ij}. (Regarding notation, repeated indices represent a sum (i.e., from 1 to 2) over that index.) The mean curvature J is then defined as

$$J = k_{\ell\ell} \tag{9}$$

Finally, the principal normal radii of curvature R_1 and R_2 are then calculated in terms of J and K as:

$$R_1, R_2 = \left| 2 \Big/ \left[J^2 \pm \left(J^2 - 4K \right)^{1/2} \right] \right| \tag{10}$$

Surface of Revolution

The tooth surface of a circular cut spiral bevel crown gear is a "surface or revolution." That is, it can be developed by rotating a curve in the shape of the cutter profile, about a fixed axis. Consider, for example, the curve C shown in Fig. 1. If C is rotated about the Z-axis, it generates a surface of revolution S, a portion of which can be considered as

the surface of a circular cut spiral bevel crown gear. Let C be defined by the expression:

$$z = f(r) \tag{11}$$

where r is the distance from the Z-axis to a typical point P on C. Let ϕ be the angle between the Z-axis and the normal line N of S at P. Then r and ϕ are dependent upon each other. That is,

$$r = r(\phi) \tag{12}$$

Let ψ be the inclination angle of the tangent line T to C at P as shown in Fig. 1. Then ψ, ϕ, and the slope of T are related as follows:

$$dz/dr = df/dr = \tan \psi = -\tan(\pi - \psi) = -\tan \phi \tag{13}$$

Consider a top view of S as shown in Fig. 2. In this view P is seen to lie on a circle of radius r, and on a radial line R which makes an angle θ with the X-axis. Then the position vector $\underset{\sim}{P}$ of P relative to O, a fixed point on the Z-axis (see Fig. 1) is:

$$\underset{\sim}{P} = z\underset{\sim}{n}_z + r\underset{\sim}{n}_r = r\underset{\sim}{n}_r + f(r)\underset{\sim}{n}_z \tag{14}$$

where $\underset{\sim}{n}_r$ and $\underset{\sim}{n}_z$ are unit vectors parallel to R and the Z-axis. Hence, in terms of $\underset{\sim}{n}_x$, $\underset{\sim}{n}_y$, and $\underset{\sim}{n}_z$, unit vectors parallel to the X, Y, and Z axis, $\underset{\sim}{P}$ becomes:

$$\underset{\sim}{P} = r \cos\theta\, \underset{\sim}{n}_x + r \sin\theta\, \underset{\sim}{n}_y + f(r)\underset{\sim}{n}_z \tag{15}$$

Since $r = r(\phi)$, P is a function of ϕ and θ. Therefore, it is convenient to let ϕ and θ be the parameters u_1 and u_2 defining S in the parametric representation $\underset{\sim}{P} = \underset{\sim}{P}(u_1,u_2)$ of the foregoing differential geometry formulae.

From Eq. (1), the surface base vectors $\underset{\sim}{g}_1$ and $\underset{\sim}{g}_2$ become:

$$\underset{\sim}{g}_1 = \underset{\sim}{g}_\phi = (dr/d\phi)\cos\theta\ \underset{\sim}{n}_x + (dr/d\phi)\sin\theta\ \underset{\sim}{n}_y + (df/dr)(dr/d\phi)\underset{\sim}{n}_z \tag{16}$$

and

$$\underset{\sim}{g}_2 = \underset{\sim}{g}_\theta = -r\sin\theta\ \underset{\sim}{n}_x + r\cos\theta\ \underset{\sim}{n}_y \tag{17}$$

Then, from Eq. (2) the metric tensora components become:

$$g_{11} = g_{\phi\phi} = (dr/d\phi)s^2\sec^2\phi \tag{18}$$

$$g_{12} = g_{21} = g_{\phi\theta} = g_{\theta\phi} = 0 \tag{19}$$

and

$$g_{22} = q_{\theta\theta} = r^2 \tag{20}$$

where Eq. (13) has been used to simplify the expressions. Hence, from Eq. (4) the unit vector $\underset{\sim}{n}$ normal to S becomes:

$$\underset{\sim}{n} = \sin\phi\cos\ \underset{\sim}{n}_x + \sin\phi\sin\theta\ \underset{\sim}{n}_y + \cos\phi\ \underset{\sim}{n}_z \tag{21}$$

The fundamental vectors $\underset{\sim}{h}_i(i = \phi,\theta)$ and the second fundamental tensor $h_{ij}(i,j = \phi,\theta)$ are then:

$$\underset{\sim}{h}_1 = \underset{\sim}{h}_\phi = \partial\underset{\sim}{n}/\partial\phi = \cos\phi\cos\theta\ \underset{\sim}{n}_x + \cos\phi\sin\theta\ \underset{\sim}{n}_y - \sin\phi\ \underset{\sim}{n}_z \tag{22}$$

$$\underset{\sim}{h}_2 = \underset{\sim}{h}_\theta = \partial\underset{\sim}{n}/\partial\theta = -\sin\phi\sin\theta\ \underset{\sim}{n}_x + \sin\phi\cos\theta\ \underset{\sim}{n}_y \tag{23}$$

$$h_{11} = h_{\phi\phi} = -(dr/d\phi)\sec\phi \tag{24}$$

$$h_{12} = h_{21} = h_{\phi\theta} = h_{\theta\phi} = 0 \tag{25}$$

and

$$h_{22} = h_{\theta\theta} = -r \sin \phi \tag{26}$$

From Eqs. (7) and (9) the Gaussian curvature and the mean curvature become:

$$K = (\sin \phi \cos \phi)/(r\, dr/d\phi) \tag{27}$$

and

$$J = -[(\cos \phi)/(dr/d\phi) - (\sin \phi)/r] \tag{28}$$

Finally, using Eq. (10) the principal normal radii of curavture become:

$$R_1 = \left|(dr/d\phi)/\cos \phi\right| \tag{29}$$

and

$$R_2 = \left|r/\sin \phi\right| \tag{30}$$

These expressions may be expressed in terms of f by using Eq. (13). That is, since

$$\phi = -\tan^{-1}(df/dr) \tag{31}$$

then $(d\phi/dr)$ becomes

$$d\phi/dr = -(d^2f/dr^2)\Big/\left[1 + (df/dr)^2\right] \tag{32}$$

and hence, R_1 and R_2 become:

$$R_1 = \left|\left[1 + (df/dr)^2\right] \Big/ \left\{(d^2f/dr^2)\cos\left[\tan^{-1}(df/dr)\right]\right\}\right| \tag{33}$$

and

$$R_2 = \left|r/\sin\left[\tan^{-1}(df/dr)\right]\right| \tag{34}$$

APPLICATION WITH GEAR TOOTH SURFACES

An Involute Curve

Perhaps the most fundamental and theoretically satisfying of all the gear tooth shapes is that generated by an involute curve. Although it is not very practical to generate a spiral bevel gear tooth surface with a rotating cutter in the shape of an involute curve, it is nevertheless informative, as a simple illustration, to examine the surface of revolution formed by an involute curve.

Consider the involute curve C as shown in Fig. 3. It is convenient to think of C as being generated as the locus of points formed by the end P of the tangent line QP as it rolls on the base circle. Then the radius of curvature ρ of C at a typical point P is simply the length TP. It is easily seen that ρ is one of the principal radii of curvature of the surface of revolution which is obtained by revolving C about the Z-axis in Fig. 3.

To see this, consider using Eqs. (29) and (30) of the foregoing analysis. These equations require knowledge of the radial distance r as a function of the angle (see Fig. 3). To obtain $r(\phi)$ let O be that point on the Z-axis which is at the same elevation as O_c the center of the circle generating c. Then r may be expressed as:

$$r = \underset{\sim}{n}_r \cdot \underset{\sim}{QP} \tag{35}$$

The vector $\underset{\sim}{QP}$ may be written as (see Fig. 3):

$$\underset{\sim}{QP} = \underset{\sim}{QO}_c + \underset{\sim}{O}_c\underset{\sim}{T} + \underset{\sim}{TP} \tag{36}$$

or

$$\underset{\sim}{QP} = b\underset{\sim}{n}_r + a\underset{\sim}{n}_c - a\phi_c\underset{\sim}{n}_t \tag{37}$$

where b is the distance OO_c, a is the circle radius, and ϕ_c is the complement of ϕ. In terms of $\underset{\sim}{n}_r$ and $\underset{\sim}{n}_z$, $\underset{\sim}{QP}$ may be written as:

$$\underset{\sim}{QP} = [b - a\cos\phi + a(\pi/2 - \phi)\sin\phi]\underset{\sim}{n}_r + [a\sin\phi + a(\pi/2 - \phi)\cos\phi]\underset{\sim}{n}_z \tag{38}$$

Hence, from Eq. (35) r and $dr/d\phi$ become:

$$r = b - a\cos\phi + a(\pi/2 - \phi)\sin\phi \tag{39}$$

and

$$dr/d\phi = a(\pi/2 - \phi)\cos\phi \tag{40}$$

Therefore, from Eqs. (29) and (30) the principal radii of curvature of the generated surface of revolution are:

$$R_1 = \left|a(\pi/2 - \phi)\right| \tag{41}$$

and

$$R_2 = \left|b\csc\phi - a\cos\phi + a(\pi/2 - \phi)\right| \tag{42}$$

An examination of Fig. 3 shows that these expressions can be interpreted simply as:

$$R_1 = \left|\underset{\sim}{TP}\right| = R_{min} \tag{43}$$

and

$$R_2 = \left|\underset{\sim}{QP}\right| = R_{max} \tag{44}$$

Finally, it is interesting to observe that if the same analysis is carried out for an involute curve generated in the opposite direction as in Fig. 4, the corresponding surface of revolution has the principal radii of curvature:

$$R_1 = |\underset{\sim}{IP}| = R_{min} \tag{45}$$

and

$$R_2 = |\underset{\sim}{QP}| = R_{max} \tag{46}$$

These results are, of course, similar to Eqs. (43) and (44). However, in this case, the centers of curvature are on opposite sides of the surface, since the Gaussian curvature is negative.

Straight Line Profile - Normal Plane

Consider next a rotating gear tooth cutter with a straight line profile which forms a gear tooth surface with a straight line profile in the normal plane as shown in Figs. 5 and 6. Viewed as a surface of revolution, this is a cone. Its defining equation may be expressed as:

$$z = (r - R_c)\cot \theta \tag{47}$$

where θ is the pressure angle as shown in Fig. 6 and R_c is the cutter radius at the base of the tooth. From this expression dz/dr and d^2z/dr^2 are readily obtained as:

$$dz/dr = \cot \theta = \tan \phi \tag{48}$$

and

$$d^2z/dr^2 = 0 \tag{49}$$

where ϕ is the complement of θ as shown in Fig. 6. Hence, Eqs. (33) and (34) give the maximum and minimum surfce radii of curvature as:

$$R_{max} = \infty \tag{50}$$

and

$$R_{min} = |r/\cos \theta| \tag{51}$$

These results might also have been obtained by recalling that a cone is generated by straight line elements (hence, infinite radius of curvature) and that the minimum radius of curvature is the distance QP as shown in Fig. 6.

Straight Line Profile - Transverse Plane

Finally, consider a rotating cutter which generates, for a crown gear, a straight line meshing profile. Specifically, consider Fig. 7 which shows the pitch plane of a crown gear where O is the gear center and C (with X,Y coordinates H,V) is the center of the rotating cutter. Let P_m be the midpoint of the gear tooth surface and let ψ be the spiral angle.

The transverse plane is normal to the X-axis at P_m. Since O is the gear center, the X-axis is a radial line and the intersection of the transverse plane and the gear tooth surface defines the transverse meshing profile shown in Fig. 8. If θ is the transverse pressure angle, the equation of the inclined tooth profile is simply

$$z = -y \cot \theta = ky \tag{52}$$

where z and y refer to coordinates along the Z and Y axis and k is defined as $-\cot \theta$. Relative to the $\hat{X}$, $\hat{Y}$, $\hat{Z}$ axis of Fig. 7, Eq. (52) becomes

$$z = \hat{z} = k(\hat{y} + V) \tag{53}$$

In terms of $\hat{x}$, $\hat{y}$, and $\hat{z}$, the profile of the cutter radius can be expressed in general as:

$$\hat{z} = f(\hat{r}) = f\left[\left(\hat{x}^2 + \hat{y}^2\right)^{1/2}\right] \tag{54}$$

The form of f, which defines the tooth surface of revolution, may be determined by observing that the intersection of the revolution surface of the cutter with the transverse plane, must coincide with the tooth profile of Fig. 8. If R_c is the distance between C and P_m, then the $\hat{X}$ coordinate of P_m is simply $R_c \sin \psi$. Hence, by letting $\hat{x} = R_c \sin \psi$ and by matching Eqs. (53) and (54), the following relation is obtained

$$f\left[\left(R_c^2 \sin^2\psi + \hat{y}^2\right)^{1/2}\right] = k(\hat{y} + V) \tag{55}$$

Let r be defined as

$$r = \left(R_c^2 \sin^2\psi + \hat{y}^2\right)^{1/2} \tag{56}$$

Then in terms of r, $\hat{y}$ becomes

$$\hat{y} = -\left(r^2 - R_c^2 \sin^2\psi\right)^{1/2} \tag{57}$$

where the negative root is required to be consistent with the coordinate system in Fig. 7. Hence, by Eq. (55) f is determined as:

$$f(r) = k\left[V - \left(r^2 - R_c^2 \sin^2\psi\right)^{1/2}\right] \tag{58}$$

which is the equation of an hyperboloid of revolution.

The maximum and minimum radii of curvature may now be determined directly by substitution into Eqs. (33) and (34), or alternatively, into Eqs. (29) and (30). To do this, note that based on Eq. (13)

$$df/dr = -\tan \phi = -kr \Big/ \left(r^2 - R_c^2 \sin^2 \psi\right)^{1/2} \tag{59}$$

where ϕ is still defined as the angle between the tooth surface normal and the $\hat{z}$-axis. Then r and $dr/d\phi$ become

$$r = R_c \sin \psi \tan \phi \Big/ \left(\tan^2 \phi - k^2\right)^{1/2} \tag{60}$$

and

$$dr/d\phi = -k^2 R_c \sin \psi \sec^2 \phi \Big/ \left(\tan^2 \phi - k^2\right)^{3/2} \tag{61}$$

Hence, upon using Eqs. (29) and (30), R_1 and R_2 become

$$R_1 = \left| k^2 R_c \sin \psi \sin^3 \phi \Big/ \left(\tan^2 \phi - k^2\right)^{3/2} \right| \tag{62}$$

and

$$R_2 = \left| R_c \sin \psi \sec \phi \Big/ \left(\tan^2 \phi - k^2\right)^{1/2} \right| \tag{63}$$

These expressions may be written in more convenient form by expressing ϕ in terms of z. That is, by identifying z with f in Eq. (58), it is readily seen that

$$r^2 = R_c^2 \sin^2 \psi + [(kV - z)/k]^2 \tag{64}$$

Then, by Eq. (59) $\sec^2 \phi$ becomes

$$\sec^2\phi = 1 + \tan^2\phi = 1 + k^2 + [k/(kV - z)]^2 k^2 R_c^2 \sin^2\psi \qquad (65)$$

Hence, R_1 and R_2 may be written as

$$R_1 = \left| \left\{ [(kV - z)/k]^2 (1 + k^2) + k^2 R_c^2 \sin^2\psi \right\}^{3/2} \Big/ kR_c^2 \sin^2\psi \right| \qquad (66)$$

and

$$R_2 = \left| \left\{ (1 + k^2)[(kV - z)/k]^2 + k^2 R_c^2 \sin^2\psi \right\}^{1/2} \Big/ k \right| \qquad (67)$$

SUMMARY OF RESULTS

In this paper, the methods of that branch of mathematics called differential geometry were applied to determine the maximum and minimum radii of curvature for circular cut bevel gear teeth. The following results were obtained.

(1) A comparison of the foregoing analysis with that developed in Ref. [1] shows that the geometry of the circular cut spiral bevel gears is somewhat simpler than that of the theoretical logarithmic spiral gears. Also, the restriction of the foregoing analysis to crown gears is a further simplification. However, the modification of the foregoing expressions for conical gears can be obtained by following the procedures outlined in Ref. [1].

(2) The above formulae for the radii of curvature of a surface of revolution (Eqs. (29), (30), (33), and (34)) are applicable to circular cut gear surfaces of any profile. The involute profile was used as an example because of its simplicity and because of the interesting results. It should be noted, however, that the involute profile as considered above is in the

radial plane of the cutter (i.e., the normal plane) and not the transverse plane of the gear.

(3) The straight line crown profile in the transverse plane, when considered in the radial plane of the cutter (the normal plane), generates a hyperboloid. Although this is a surface of revolution, it is also a "ruled surface" since it can be considered as generated by a one-parameter family of lines. Equations (66) and (53) show that the maximum radii of curvature occurs when $z - kv$ or when $y = 0$, that is, at the pitch surface. Similarly, Eq. (66) shows that the minium radii of curvature occurs at the greatest elevation above the pitch surface.

Finally, the analysis does not consider the effect of "crowning" or other adjustments commonly made in the manufacture of spinal bevel gears. In this sense, the foregoing analysis pertains primarily to theoretical gears. The effects of crowning and geometrical variations due to grinding and lapping needs additional study.

REFERENCES

1. Huston, R. L., and Coy, J. J., "Ideal Spiral Bevel Gears - A New Approach to Surface Geometry," ASME Journal of Mechanical Design, Vol. 103, No. 1, Jan. 1981, pp. 127-133.

2. Buckingham, E., Analytical Mechanics of Gears, Dover Publications, New York, 1963, pp. 338-351.

3. Dudley, D. W., ed., Gear Handbook, 1962, Chapter 20.

4. Dallas, D. B., ed., Tool and Manufacturing Engineers Handbook, 3rd ed., McGraw Hill, New York, 1976, Chapter 11.

5. Bonsignore, A. T., "The Effect of Cutter Diameter on Spiral Bevel Tooth Proportions," American Gear Manufacturers Association, Paper No. AGMA 124.20, October 1976.

6. Krenzer, T. J., "The Effect of Cutter Radius on Spiral Bevel and Hypoid Tooth Contact Behavior," American Gear Manufacturers Association, Paper No. AGMA 129.21, October 1976.

7. Watson, H. J. Modern Gear Production, Pergamon Press, Oxford, 1970, Chapter 8.

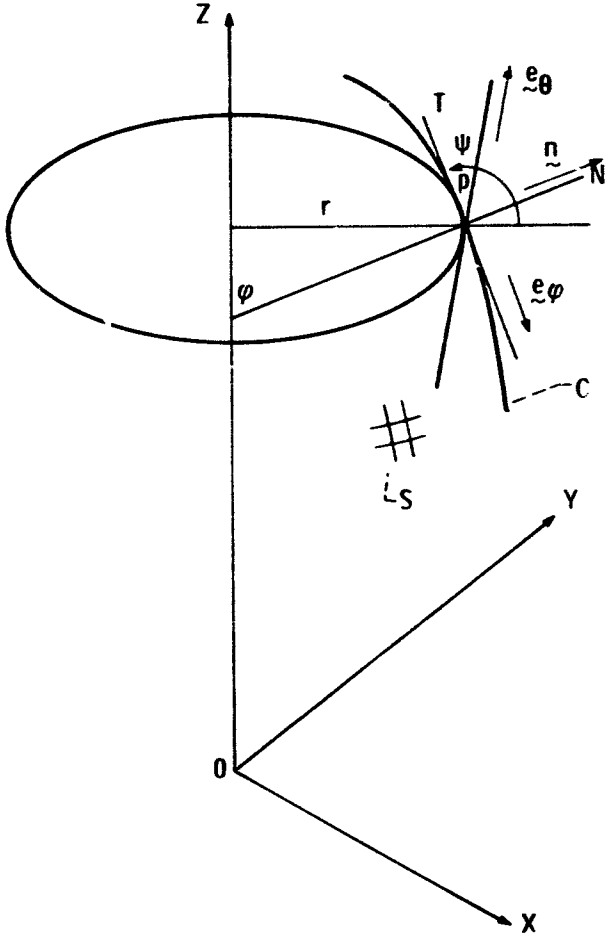

Figure 1. - A surface of revolution about the Z-axis.

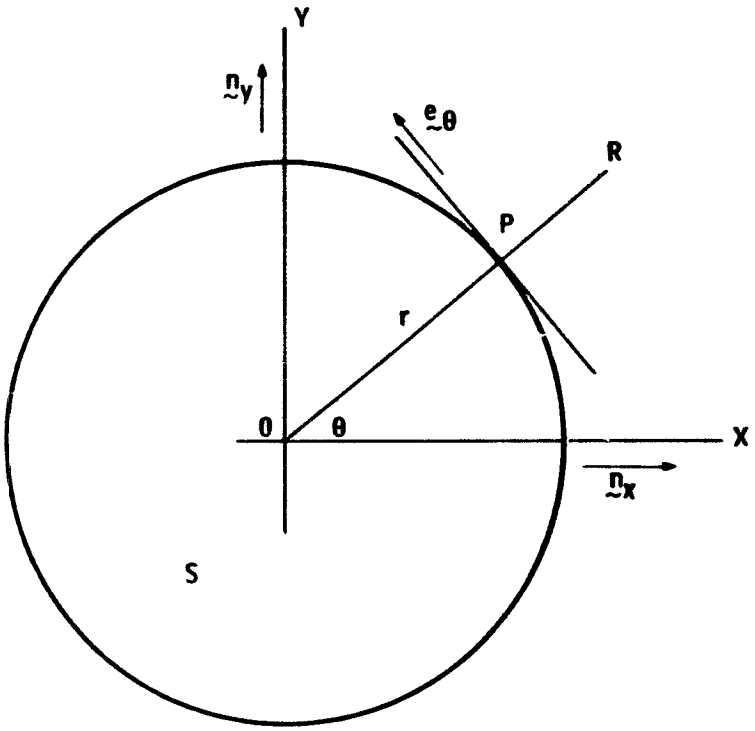

Figure 2. - Top view of a surface of revolution.

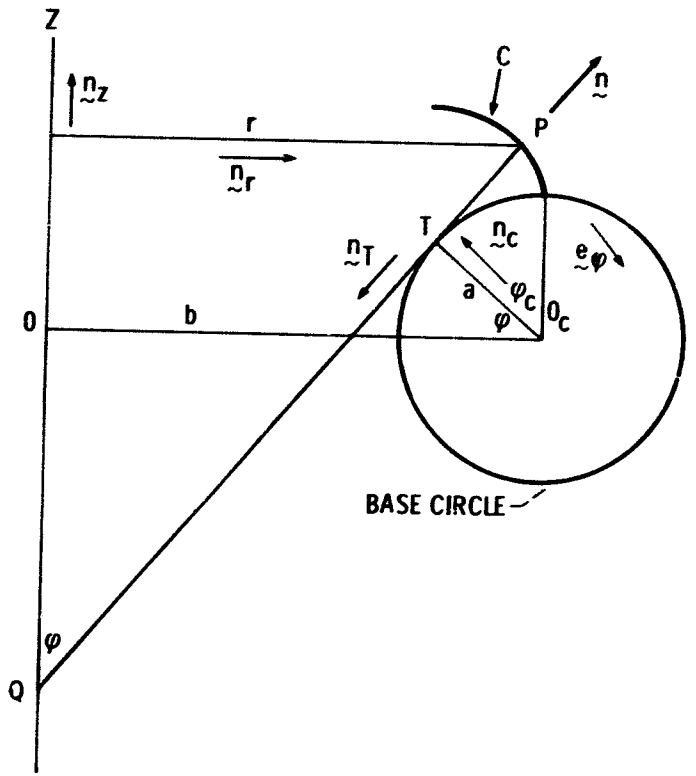

Figure 3. - An involute curve as a generator for a surface of revolution.

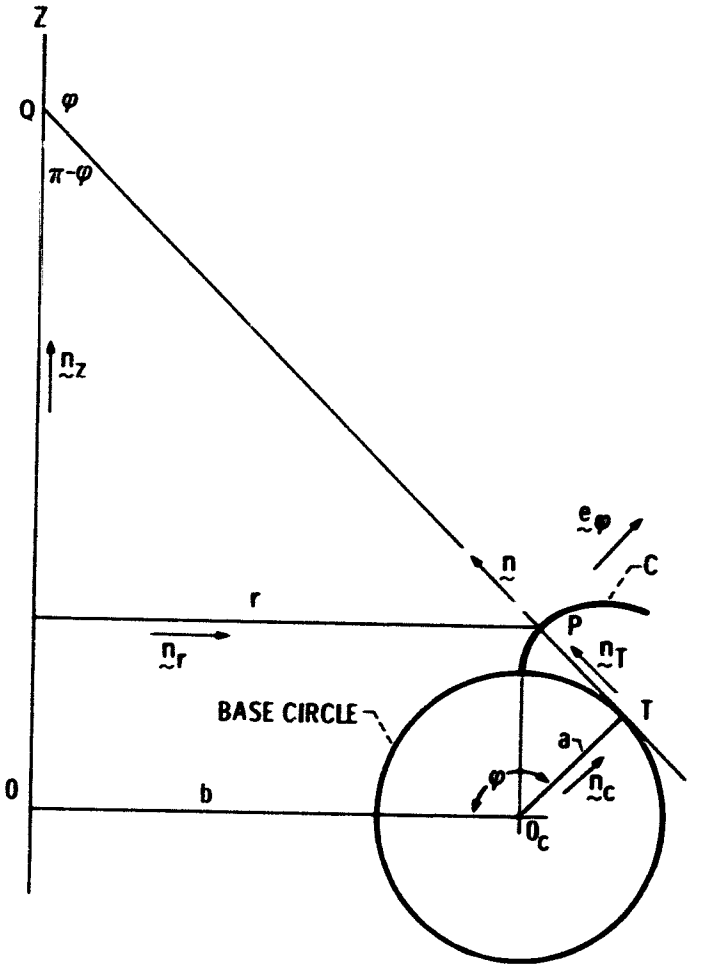

Figure 4. - A second involute curve as a generator for a surface of revolution.

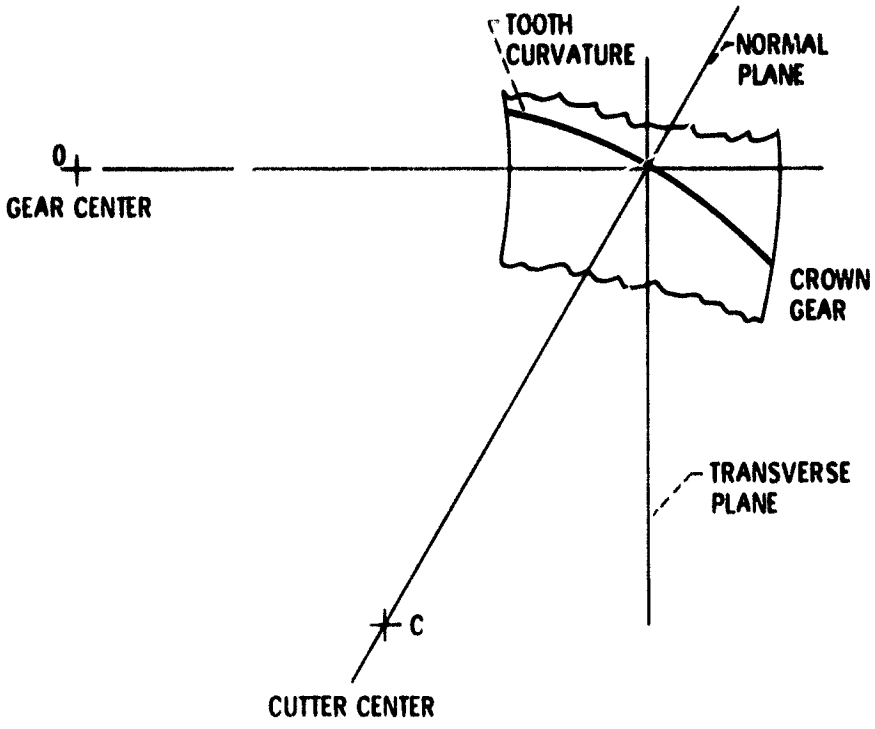

Figure 5. - Top view showing gear and cutter centers and edge view of normal and transverse planes.

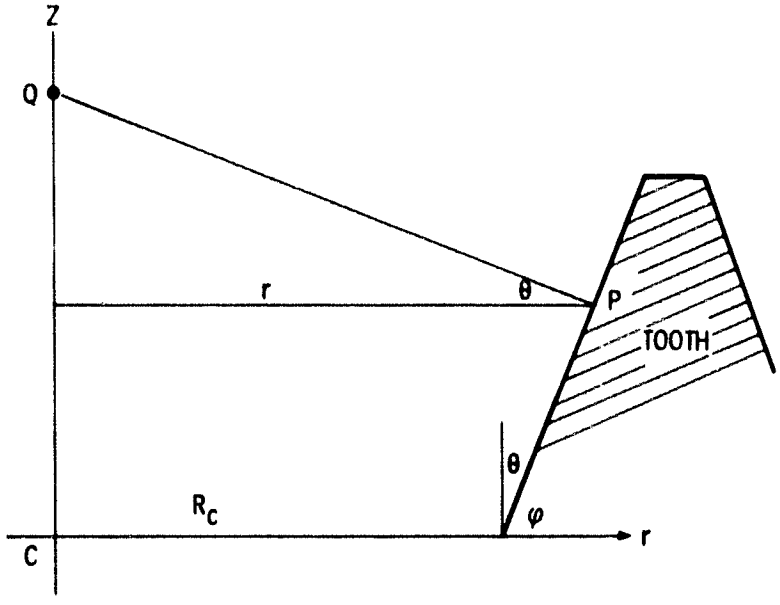

Figure 6. - True view of normal plane showing crown gear tooth profile.

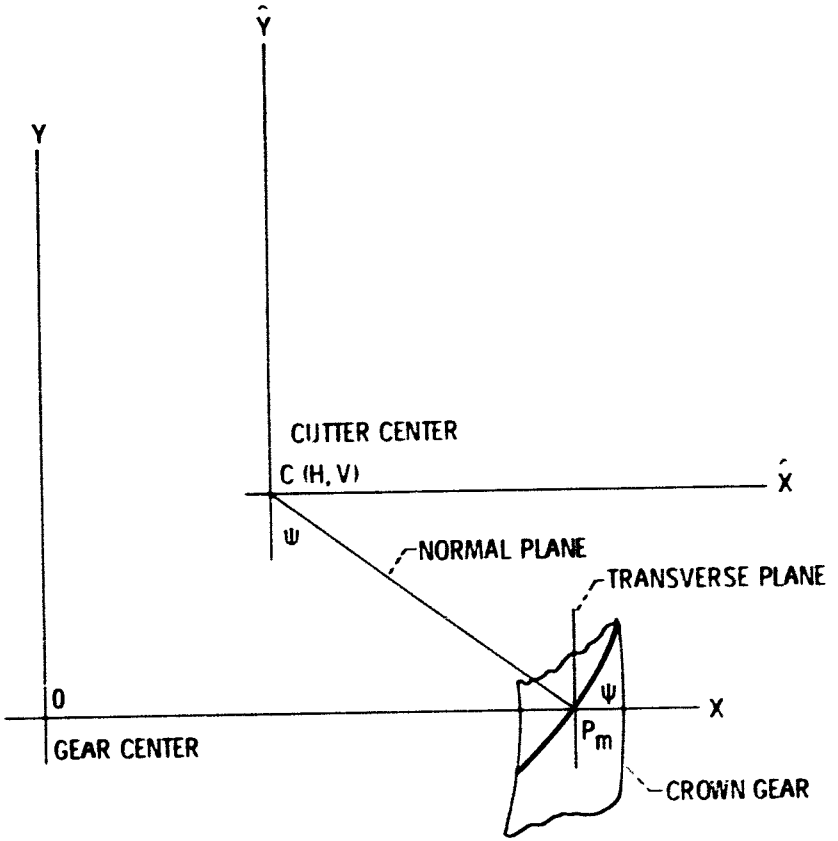

Figure 7. - View of crown gear in pitch plane.

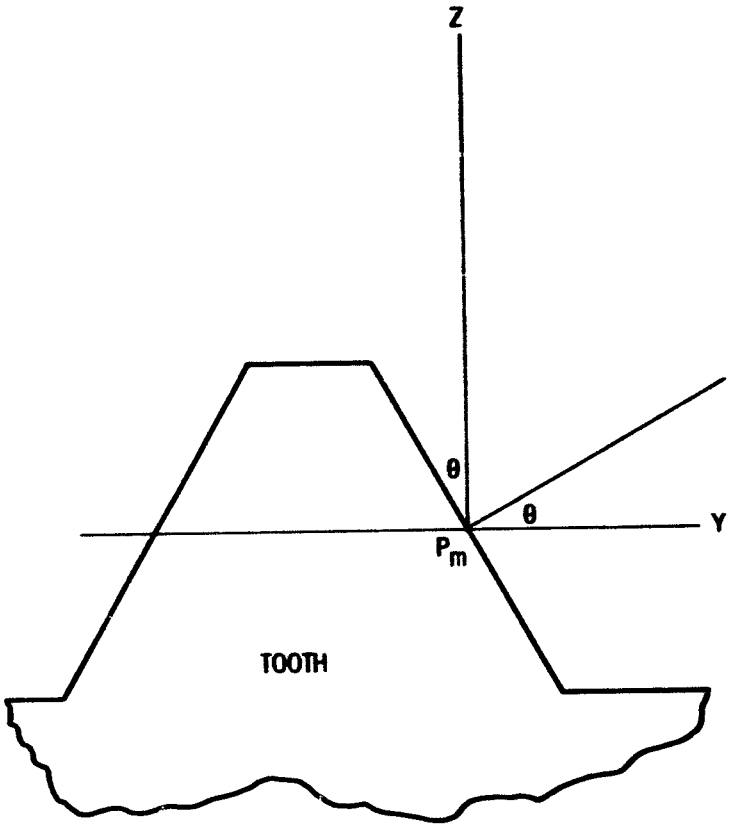

Figure 8. - True view of transverse plane showing crown tooth profile.